Nature of the Modifying Action of White Phosphorus on the Properties of Nanosized Hydrogenation Catalysts Based on Bis(dibenzylideneacetone)palladium(0)

L. B. Belykh*, N. I. Skripov, L. N. Belonogova, V. A. Umanets, T. P. Stepanova, and F. K. Schmidt

Irkutsk State University, Irkutsk, 664033 Russia
e-mail: belykh@chem.isu.ru

Received December 17, 2010

Abstract—The catalytic properties and nature of the nanoparticles forming in the system based on $Pd(dba)_2$ and white phosphorus are reported. A schematic mechanism is suggested for the formation of nanosized palladium-based hydrogenation catalysts. The mechanism includes the formation of palladium nanoclusters via the interaction of $Pd(dba)_2$ with the solvent (N,N-dimethylformamide) and substrate and the formation of palladium phosphide nanoparticles. The inhibiting effect exerted by elemental phosphorus on the catalytic process is due to the conversion of part of the $Pd(0)$ into palladium phosphides, which are inactive in hydrogenation under mild conditions, and the formation of mainly segregated palladium nanoclusters and palladium phosphide nanoparticles. By investigating the interaction between $Pd(dba)_2$ and white phosphorus in benzene, it has been established that the formation of palladium phosphides under mild conditions consists of the following consecutive steps: $Pd(0) \rightarrow PdP_2 \rightarrow Pd_5P_2 \rightarrow Pd_3P$. It is explained why white phosphorus can produce diametrically opposite effects of on the catalytic properties of nanosized palladium-based hydrogenation catalysts, depending on the nature of the palladium precursor.

DOI: 10.1134/S002315841105003X

A central problem of catalytic chemistry is that of elucidating the nature, regularities of formation, and the ways of functioning and deactivation of catalytically active particles. Without understanding these issues, it is impossible to devise a purposeful approach to design of high-efficiency catalytic systems and to preparation of new catalysts. Earlier, we demonstrated that not only phosphines, but also elemental phosphorus can serve as an effective promoter for nanosized palladium-based hydrogenation catalysts prepared under the action of molecular hydrogen [1—3]. The introduction of white phosphorus prior to the reduction of the palladium precursor PdX_2 raises, by a factor of 4 to 9 at P : Pd = 0.3 mol/mol, the turnover frequency (X = acac, OAc) and/or turnover number (X = acac, OAc, Cl) of the reaction catalyzed by the resulting nanoparticles. The strong promoting effect observed at small P : Pd ratios (X = acac) is due to the increase in the degree of dispersion of the catalyst, for which the following model was suggested: the core of the nanoparticle consists of palladium phosphides, mainly Pd_6P, and the surface of the nanoparticles consists of hydrogenation-active $Pd(0)$ clusters. However, depending on the acido ligand in the precursor, on the reducing agent, and on the modifier concentration, elemental phosphorus exerts either a promoting or an inhibiting effect on palladium catalysts [3]. We believe that this is due to the variation of the ratios between the rate of precursor reduction to $Pd(0)$, the $Pd(0)$ clustering rate, and the rate of the interaction between $Pd(0)$

and P_4 and, accordingly, the variation of the nature of the resulting nanoparticles.

For chemical modeling of particular stages of the formation of palladium-based hydrogenation catalysts modified with elemental phosphorus, we studied the interaction between bis(dibenzylideneacetone)palladium(0) ($Pd(dba)_2$) and white phosphorus and the catalytic properties of the resulting system. $Pd(dba)_2$ was chosen for the following reasons: firstly, this precursor needs no reduction in the preparation of catalytically active particles; secondly, dibenzylideneacetone is the most labile among the known π ligands and can readily be displaced from the coordination sphere of the metal. At the same time, unlike phosphines, this ligand does not undergo destruction in the coordination sphere of palladium.

EXPERIMENTAL

Solvents (benzene and N,N-dimethylformamide (DMF)) were purified by standard methods used in organometallic chemistry [4]. For dehydration and amine removal, DMF was held over anhydrous copper sulfate until the formation of a green solution and was distilled twice in vacuo (8 Torr) at a temperature not higher than 42°C. Benzene was distilled from $LiAlH_4$ for deeper dehydration and was stored in an argon atmosphere over molecular sieve 4A in sealed tubes. As determined by the Fischer method [5], the water con-

tent of benzene was 1.1×10^{-3} mol/l and that of DMF was 0.8 mol/l.

Dibenzylideneacetone (dba) was synthesized by reacting benzaldehyde with acetone [6] followed by the recrystallization of the product from ethanol. ^{1}H NMR (CDCl$_3$, δ, ppm): 7.76 (2H$_A$, d, ^3J = 16 Hz) and 7.11 (2H$_B$, d, ^3J = 16 Hz). ^{13}C NMR (CDCl$_3$, δ, ppm): 189.4 (CO), 143.8 (C1, d, $^1J_{CH}$ = 154 Hz), 125.8 (C2, d, $^1J_{CH}$ =158 Hz), 135.9 (1C, Ph), 129.7 (2C, o-Ph), 130.1 (2C, m-Ph), and 131.4 (1C, p-Ph).
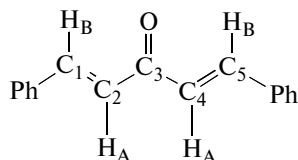
Bis(dibenzylideneacetone)palladium(0) (Pd(dba)$_2$) was synthesized by PdCl$_2$ reduction with methanol in the presence of sodium acetate and dibenzylideneacetone [7, 8]. Dibenzylideneacetone (3.4500 g, 1.472 × 10^{-2} mol), sodium acetate trihydrate (4.8525 g, 3.568 × 10^{-2} mol), and methanol (113 ml) were placed in a two-neck round-bottom flask in an argon atmosphere. The mixture was stirred at 50°C for 45–60 min, and PdCl$_2$ (0.7875 g, 4.434 × 10^{-3} mol) was added to the resulting solution. The reaction solution was stirred in an argon atmosphere at 40°C for 4 h. The resulting dark violet precipitate was collected on a Schott filter and was washed with water and acetone. The solid was dried in vacuo (30°C, 2–3 Torr) for 3 h. Yield: 2.4 g (94% of the theoretical value); mp 152°C. Pd(dba)$_2$, which exists in solution as the dimer Pd$_2$(dba)$_3$Solv), contains three bridging bidentate dibenzylideneacetone ligands in the s-cis–s-$trans$ conformation. ^{1}H NMR (CDCl$_3$, δ, ppm): dba (1): cis-alkene—6.65 (H$_A$, d, ^3J = 13.4 Hz) and 6.77 (H$_B$, d, ^3J = 13.4 Hz); $trans$-alkene—4.99 (H$_A$, d, ^3J = 13.4 Hz) and 5.94 (H$_B$, d, 3J = 13.4 Hz); dba (2): cis-alkene—6.37 (H$_A$, d, ^3J = 13.4 Hz) and 6.47 (H$_B$, d, 3J = 13.4 Hz); $trans$-alkene—4.96 (H$_A$, d, ^3J = 13.4 Hz) and 5.89 (H$_B$, d, ^3J = 13.4 Hz); dba (3): cis-alkene—5.13 (H$_A$, d, ^3J = 13.4 Hz) and 5.34 (H$_B$, d, ^3J = 13.4 Hz); $trans$-alkene—6.16 (H$_A$, d, ^3J = 12.2 Hz) and 6.81 (H$_B$, d, ^3J = 12.2 Hz); dba (free): 7.76 (2H$_A$, d, ^3J = 16 Hz) and 7.11 (2H$_B$, d, ^3J = 16 Hz) [9]. ^{13}C NMR (CDCl$_3$, δ, ppm): 184.9 (CO), 182.2 (CO), 181.1 (CO), 111.3 (d, $^1J_{CH}$ = 160 Hz), 108.2 (d, $^1J_{CH}$ = 158 Hz), 107.9 (d, $^1J_{CH}$ = 157 Hz), 94.6 (d, $^1J_{CH}$ = 160 Hz), 89.8 (d, $^1J_{CH}$ = 158 Hz), and 85.6 (d, $^1J_{CH}$ = 159 Hz); dba (free): 189.4 (CO), 143.8 (d, $^1J_{CH}$ = 154 Hz), and 125.8 (d, $^1J_{CH}$ = 154 Гц). Here, cis- and $trans$-alkene designate the alkene moieties of dibenzylideneacetone that are, respectively, cis and $trans$ to the carbonyl group.

White phosphorus was mechanically purified from surface oxidation products and was washed with dehydrated benzene immediately before use. A benzene solution of white phosphorus was prepared and stored in an inert atmosphere in a finger-shaped vessel whose design allowed it to be vacuumized and filled with argon. ^{31}P NMR: δ = −522 ppm (s).

The reaction between bis(dibenzylideneacetone)palladium(0) and white phosphorus was carried out at different reactant ratios in a benzene medium under dry, deoxygenated argon in a finger-shaped vessel.

Example 1. A benzene solution of white phosphorus (9.4 ml, 18.8 × 10^{-4} mol) was added to a burgundy solution of Pd(dba)$_2$ (0.5405 g, 9.4 × 10^{-4} mol) in 210 ml of benzene. As the solution of elemental phosphorus was being added, the color of the solution changed quickly from burgundy to black. In 10−20 s, a black solid precipitated and the solution turned yellow. After the completion of the reaction, the solution was separated from the precipitate by decantation. The solution was analyzed by ^{31}P NMR and UV spectroscopy. The precipitate (sample **1**) was washed with benzene (10 ml) three times and was dried in vacuo (30°C, 1 Torr). Yield: 0.16 g. Sample **1** was X-ray-amorphous. It was crystallized by heat treatment at 400°C in an inert atmosphere in a sealed tube for 4 h and was then cooled slowly. The X-ray diffraction pattern of crystallized sample 1 showed the following reflections (d/n, Å (I/I_0)): 4.004(46), 3.340(15), 2.998(31), 2.930(65), 2.878(94), 2.722(100), 2.515(29), 2.448(15), 2.284(32), 2.122(31), 2,111(37), 2.080(38), 2.052(38), 2.002(35), 1.982(15), 1.900(23), 1.838(33), 1.795(31), 1.735(23), 1.689(20), 1.489(15), 1.470(25), 1.367(15), 1.349(11), and 1.308(11) (hereafter, the numbers in parentheses are relative reflection intensities). The reflections at 2.930, 2.878, 2.722, 2.515, 2.052, 2.002, 1.900, 1.689, 1.470, and 1.349 Å are consistent with the X-ray diffraction data for the palladium phosphide PdP$_2$ [10]. The reflections at 3.340, 2.722, 2.515, 2.448, 2.284, 2.122, 2.111, 2.080, 1.982, 1.838, 1.735, 1.470, 1.367, 1.349, and 1.308 Å are consistent with the X-ray diffraction data for the palladium phosphide Pd$_5$P$_2$ (PDF 19-887) [11]. The reflections at 4.004, 2.998, and 1.489 Å were not assigned to any phase.

Example 2. A benzene solution of white phosphorus (4 ml, 2.4 × 10^{-4} mol) was added to a burgundy solution of Pd(dba)$_2$ (0.69 g, 1.2 × 10^{-3} mol) in 260 ml of benzene. A black precipitate formed at the early stages of the reaction, but the solution retained its burgundy color. The solution was analyzed by ^{31}P NMR and UV spectroscopy. After 6 days, the solution was separated from the precipitate by decantation. The solid (sample **2**) was washed with benzene (10 ml) three times and was dried in vacuo (30°C, 1 Torr). Yield: 0.15 g. Sample **2** was a combination of crystalline and amorphous phases. The X-ray diffraction pattern of sample **2** showed, in a scattering angle range of $2θ = 30°−75°$ and against the background of an amorphous halo at $2θ = 35°−45°$, the following reflections from a crystalline phase (d/n, Å (I/I_0)): 2.910(8), 2.871(24), 2.796(6), 2.739(17), 2.667(5), 2.623(15), 2.548(7), 2.505(28), 2.473(15), 2.420(18), 2.362(28), 2.320(34), 2.288(40), 2.247(53), 2.222(47), 2.188(35), 2.168(27), 2.118(24), 2.100(22), 2.075(20), 2.068(20), 2.044(16), 2.022(12), 1.987(11), 1.958(11), 1.933(11), 1.920(11), 1.902(10), 1.882(6), 1.880(4), 1.837(7), 1.802(4), 1.779(4), 1.767(4), 1.749(4), 1.714(2), 1.680(2),

Monitoring data for the decomposition of the $Pd(dba)_2$ complex in DMF in an inert atmosphere

Time, min	$Pd(dba)_2$ concentration		dba concentration, mmol/l
	mmol/l	%	
20	0.711	71.1	0.59
60	0.570	57.0	0.90
90	0.313	31.2	1.36
120	0.164	16.4	1.74
150	0.095	9.5	1.93
180	0	0	2.06

Note: $C_{Pd(dba)_2} = 1$ mmol/l, 30°C.

1.595(2), 1.519(2), 1.454(1), 1.374(4), 1.366(4), and 1.318(7). The reflections at 2.910, 2.871, 2.739, 2.505, 2.044, 1.987, 1.902, 1.714, 1.454, 1.366, and 1.318 Å are consistent with the X-ray diffraction data for PdP_2 [10]. The reflections at 2.667, 2.548, 2.505, 2.362, 2.320, 2.288, 2.247, 2.222, 2.118, 2.100, 2.075, 1.987, 1.882, 1.880, 1.837, 1.779, 1.767, 1.749, 1.680, 1.595, 1.519, 1.454, and 1.374 Å are consistent with the X-ray diffraction data for the palladium phosphide $Pd_{12}P_{3.2}$ (PDF 42-0922) [11]. The formula of the palladium phosphide $Pd_{12}P_{3.2}$ is also written as $Pd_3P_{0.8}$. The reflections at 2.796, 2.623, 2.548, 2.505, 2.420, 2.362, 2.320, 2.247, 2.222, 2.168, 2.118, 2.075, 2.068, 2.022, 1.987, 1.958, 1.933, 1.902, 1.882, 1.880, and 1.802 Å are consistent with the X-ray diffraction data for the palladium phosphide $Pd_{4.8}P$ (PDF 19-0890) [11]. It is possible that palladium was present in the sample (d/n, Å (I/I_0): 2.247, 1.958, and 1.374). Some reflections at small scattering angles were not identified.

Catalytic hydrogenation was performed in a temperature-controlled glass shaker at 30°C and an initial hydrogen pressure of 1 atm in the presence of a palladium catalyst obtained in situ. The catalyst was prepared as follows. A DMF solution of $Pd(dba)_2$ (1.1 mmol/l, 9 ml) was placed in a finger-shaped vessel in an inert atmosphere, and 1 ml of a benzene solution of white phosphorus was added in drops (P : Pd = 0.2–1.5). The solution was agitated for 10 min at room temperature and was then transferred into a prevacuumized and hydrogen-filled shaker. The shaker was closed with a Teflon stopper with a rubber septum, a hydrogen pressure of 2 atm was established, and the substrate (styrene) was syringed into the reaction mixture. Hydrogenation was conducted under vigorous agitation to rule out diffusion control of the reaction. The reaction was monitored as the pressure drop measured with a manometer, as well as by GLC on a Chrom-5 chromatograph (3.6-m-long column packed with Carbowax 20M, flame-ionization detector).

UV spectra were recorded on an SF-2000 spectrophotometer using a sealed cuvette (light path length of 0.01 cm). The $Pd(dba)_2$ concentration was calculated from the intensity of the absorption band at 525 nm ($d \rightarrow d^*$-transition, $\varepsilon_{525} = 6400$ l mol^{-1} cm^{-1}); the dibenzylideneacetone concentration, from the intensity of the absorption band at 325 nm ($n \rightarrow \pi^*$ transition, $\varepsilon_{325} = 41\ 280$ l mol^{-1} cm^{-1}) [12], with the absorbance of the $Pd(dba)_2$ complex at this wavelength ($n \rightarrow \pi^*$-transition, $\varepsilon_{325} = 33\ 540$ l mol^{-1} cm^{-1}) taken into account.

NMR spectra were recorded on a VXR-500S pulsed spectrometer (Varian). ^{31}P chemical shifts are reported relative to 85% orthophosphoric acid, with positive values corresponding to downfield shifts. ^{13}C and ^1H chemical shifts are reported relative to tetramethylsilane.

Catalyst samples were characterized by X-ray diffraction on a DRON-3M diffractometer (CuK_α radiation). Catalysts were also examined by transmission electron microscopy (TEM) on a Philips EM-410 microscope. A drop of a catalyst solution prepared in situ was placed on a carbon-coated specimen grid and was dried in an argon atmosphere. The imaging conditions ruled out the melting or decomposition of the specimen under the action of the electron beam.

RESULTS AND DISCUSSION

The palladium catalyst based on the $Pd(dba)_2$ complex in the DMF medium is active in the hydrogenation of terminal bonds of alkenes, including styrene, under mild conditions. The maximum value of the turnover frequency of the catalyst is 270 (mol styrene) (mol Pd)$^{-1}$ min^{-1}, and the turnover number is 5235 (mol styrene)/(mol Pd). UV spectroscopic data demonstrated that, after styrene hydrogenation is complete, the reaction mixture contains neither the initial palladium(0) complex nor free dibenzylideneacetone; that is, srtyrene hydrogenation is accompanied by dibenzylideneacetone hydrogenation. The maximum catalytic activity in styrene hydrogenation, as calculated from the initial rate of the reaction, decreases from 270 to 100 and 60 (mol styrene) (mol Pd)$^{-1}$ min^{-1} if the DMF solution of $Pd(dba)_2$ is used 2 and 4 h after preparation, respectively. The UV spectroscopic study of bis(dibenzylideneacetone)palladium(0) conversion in DMF showed the $Pd(dba)_2$ concentration decreases with time and, in 3 h, $Pd(dba)_2$ at 30°C turns entirely into palladium nanoclusters, leaving free dibenzylideneacetone in the solution (table).

The decrease in the $Pd(dba)_2$ concentration upon the dissolution of the complex in DMF is due to the displacement of coordinated dibenzylideneacetone by DMF molecules, which cannot stabilize Pd(0) complexes. The decomposition of $Pd(dba)_2$ in DMF at 30°C is described by a pseudo-first-order rate equation:

$$w = k_1 C_{Pd(dba)_2},$$

where w is the reaction rate, k_1 is the rate constant (min^{-1}), and C is the current $Pd(dba)_2$ concentration. The k_1 value is 1.28×10^{-2} min^{-1}.

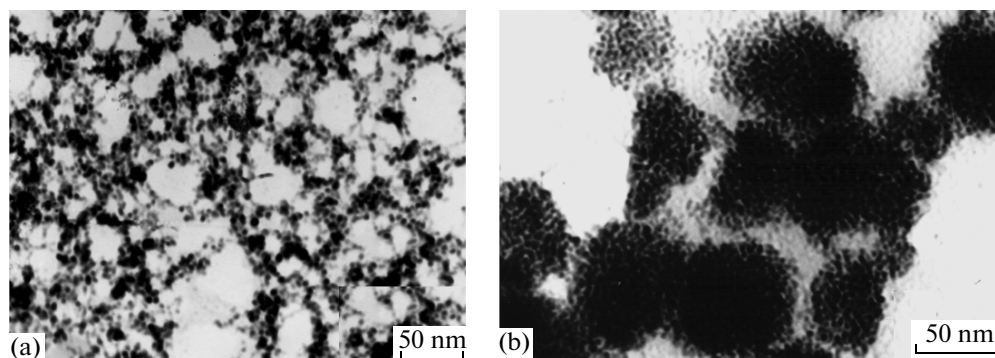**Fig. 1.** TEM images of the (a) Pd(dba)$_2$−DMF and (b) Pd(dba)$_2$−styrene−DMF systems. C_{Pd} = 1 mmol/l, 30°C, P_{Ar} = 1 atm.

The resulting palladium nanoclusters, whose average size is ~3 nm, according to TEM data, are prone to aggregation and interact to form branched chains (Fig. 1a).

Thus, when the Pd(dba)$_2$ complex in DMF is used as the precursor, the solution before the hydrogenation stage may contain both the initial palladium(0) complex and palladium nanoclusters.

It was demonstrated by additional experiments that, upon the introduction of styrene into the DMF solution of Pd(dba)$_2$ in an inert atmosphere, the solution changes its color from burgundy through greenish yellow to brown within a few seconds and turns into a colloidal solution. The self-organization of base palladium nanoparticles ~3 nm in size yields spherical 60- to 70-nm supramolecular structures (Fig. 1b). A similar situation was observed earlier for the nanosized hydrogenation catalyst forming in the PdCl$_2$−P−H$_2$ system [3].

The formation of two types of supramolecular structures may be due to the rate-limiting steps of their formation being different. Both in the diffusion-controlled aggregation model and in the cluster−cluster aggregation model, the rate-limiting step of the formation of fractal structures is the diffusion of base nanoparticles, with the probability of sticking of primary particles being unity [13, 14]. If the rate-limiting step is particle growth, then the weak sticking of base particles to one another will be favorable for deeper interpenetration of primary particles and for the formation of more compact aggregates.

Our experimental data indicate that the catalytic activity observed in the case of Pd(dba)$_2$ as the precursor is due not to the palladium(0) complex itself, but to the palladium nanoclusters. Note that no example of the participation of mononuclear Pd(0) complexes in hydrogenation catalysis has been reported to date. Once nanoparticles have formed in the system, hydrogenation will take place on their surface [15].

The addition of white phosphorus to the DMF solution of Pd(dba)$_2$ changes the catalytic properties of the system. The catalytic activity of the Pd(dba)$_2$−P

system in styrene hydrogenation decreases nearly linearly with an increasing modifier concentration (Fig. 2). A similar trend was observed earlier for the PdCl$_2$−P−H$_2$ system [3]. By contrast, with Pd(acac)$_2$ or Pd(OAc)$_2$ as the precursor, the catalytic activity increases with an increasing modifier concentration and passes through a maximum at P : Pd = 0.3 [2]. The hydrogenation activity at this point is 280 (mol substrate) (mol Pd)$^{-1}$ min^{-1}, one order of magnitude higher than the activity of the unmodified system.

In order to obtain an experimental substantiation for the inhibiting effect of white phosphorus on the catalytic properties of palladium nanoclusters, we studied the products of the interaction between Pd(dba)$_2$ and elemental phosphorus. According to TEM data, high-contrast particles form in the Pd(dba)$_2$−P system in DMF. Their average size is 2.7 nm at P : Pd = 0.3 (Fig. 3).

The fact that the high-contrast particles forming in the absence of phosphorus and those forming in the presence of P$_4$ are similar in size suggests that the inhibiting effect of elemental phosphorus on the catalytic properties of the Pd(dba)$_2$-based system is associated with the nature of the resulting high-contrast nanoparticles rather than with their size.

It was demonstrated earlier that white phosphorus can react with Pd(II) compounds under mild conditions to yield palladium phosphides of different compositions, which are inactive in hydrogenation under mild conditions [2]. Taking this fact into consideration, we investigated the interaction between Pd(dba)$_2$ and white phosphorus at varied reactant ratios. To rule out the conversion of bis(dibenzylideneacetone)palladium(0) into palladium nanoclusters, which would take place in DMF, we conducted the interaction between Pd(dba)$_2$ and elemental phosphorus in benzene, in which Pd(dba)$_2$ at a concentration of about 3.0 mmol/l is stable over 24 h.

According to ^{31}P NMR and UV spectroscopic data, the reaction between Pd(dba)$_2$ and elemental phosphorus in benzene in an inert atmosphere takes place fairly readily at room temperature. At P : Pd = 2
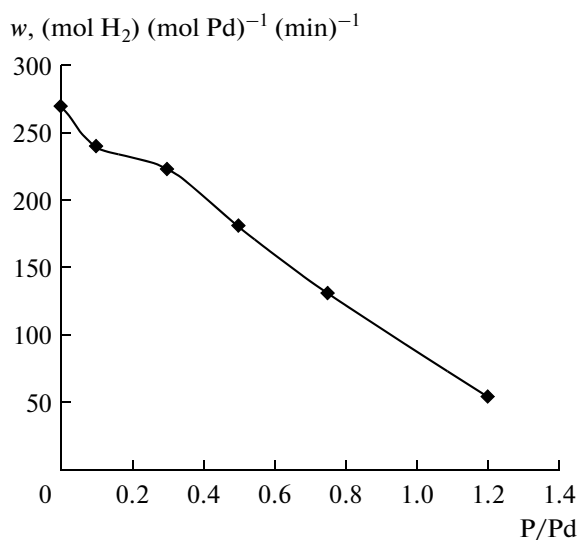
Fig. 2. Catalytic activity of the Pd(dba)$_2$–P system in styrene hydrogenation as a function of the reactant ratio. C_{Pd} = 1 mmol/l, [Ph–CH=CH$_2$]: [Pd(dba)$_2$] = 873, DMF, 30°C, P_{H_2} = 1 atm.
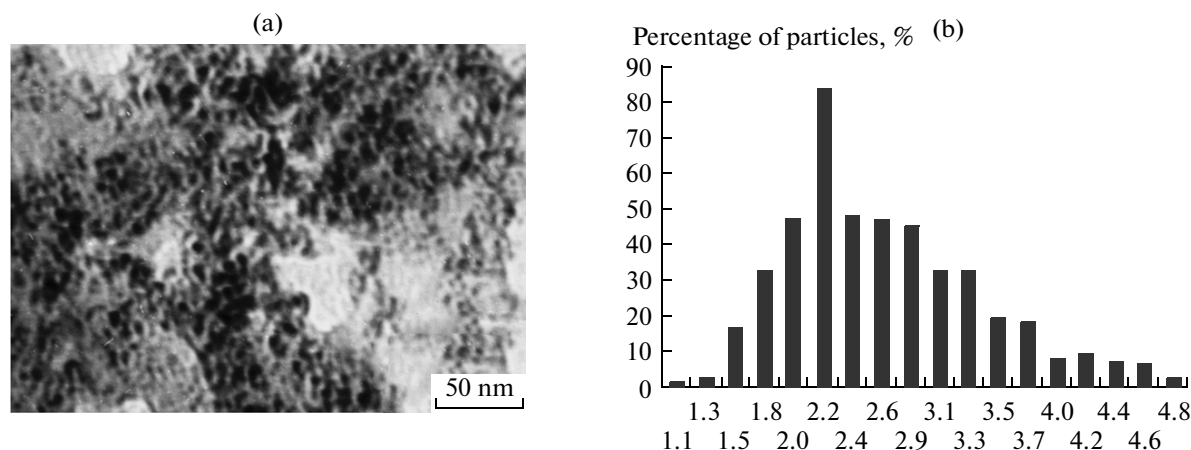
Fig. 3. (a) TEM image of the Pd(dba)$_2$–0.3P system in DMF; C_{Pd} = 1 mmol/l, 30°C, P_{H_2} = 1 atm. (b) Particle size distribution.

($C_{Pd(dba)_2}$ = 3.280 mmol/l), the reaction is complete within 10–20 s, yielding a black precipitate (sample **1**). The dibenzylideneacetone concentration at this point is 5.864 mmol/l, as calculated from the UV spectrum of the reaction system; therefore, nearly the entire dibenzylideneacetone of the Pd(dba)$_2$ complex remains in the solution. The absence of the resonance signal from white phosphorus (^{31}P NMR: δ = −522 ppm) in the ^{31}P NMR spectrum of the Pd(dba)$_2$–2P system recorded 10 min after the beginning of the reaction and the absence of resonances due to phosphorus conversion products between +500 and −550 ppm indicate that elemental phosphorus is incorporated in sample **1**.

According to X-ray diffraction data, sample 1 (P : Pd = 2) is an X-ray amorphous substance (Fig. 4, curve *a*). After it is heat-treated in an inert atmosphere (400°C, 4 h), its diffraction pattern shows broad reflections from the crystalline palladium phosphides PdP$_2$ and Pd$_5$P$_2$, the PdP$_2$ phase being dominant (Fig. 4, curve *b*). Therefore, the reaction between Pd(dba)$_2$ and white phosphorus in benzene at P : Pd = 2 mainly yields PdP$_2$, the palladium phosphide richest in phosphorus.

At reactant ratios of P : Pd < 2 (P : Pd = 0.4 and 1), complete or nearly complete Pd(dba)$_2$ conversion in the Pd(dba)$_2$–nP system is also possible, but, according to UV spectroscopic data, the reaction time increases
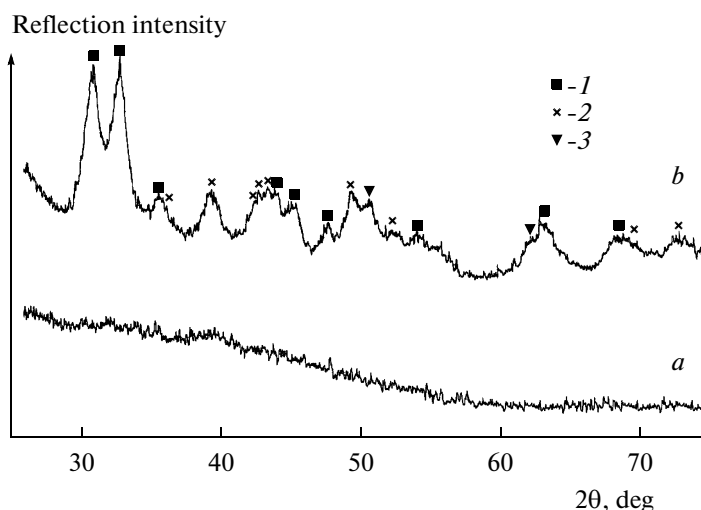
Fig. 4. X-ray diffraction patterns of sample **1** (P : Pd(dba)$_2$ = 2) (*a*) before and (*b*) after heat treatment in argon (400°C, 4 h): (*1*) PdP$_2$, (*2*) Pd$_5$P$_2$, and (*3*) unidentified phase.

from 10–20 s at P : Pd = 2 to 3 h at P : Pd = 1.0 and to 24 h at P : Pd = 0.4 (90% conversion). At P : Pd = 0.2, the Pd(dba)$_2$ conversion is only 70% in 6 days. Note that the ^{31}P NMR spectra of the Pd(dba)$_2$–*n*P reaction systems with *n* = 0.2 and 1.0, like the spectrum recorded for P : Pd = 2, show no resonance from white phosphorus (δ = −522 ppm) as soon as 10 min after the beginning of the reaction, and no other signals between +500 and −550 ppm are observed either at the early stages of the reaction or in 1 day.

The Pd(dba)$_2$ concentration versus time curves indicate two distinct kinetic regions for the palladium complex–white phosphorus interaction (Fig. 5). In the first (initial) region, the reaction rate as a function of the white phosphorus concentration changes from 1.1×10^{-4} mol l^{-1} min^{-1} for P : Pd = 0.2 to 2.04×10^{-4} mol l^{-1} min^{-1} for P : Pd = 0.4 and 4.54×10^{-4} mol × × l^{-1} min^{-1} for P : Pd = 1.0, suggesting that the reaction is first-order with respect to phosphorus. In the second kinetic region, the reaction rate is lower by a factor of 15–40. The totality of spectroscopic and kinetic data suggests that, at the initial stages, the reaction between Pd(dba)$_2$ and white phosphorus yields PdP$_2$ at various reactant ratios. The further conversion of Pd(dba)$_2$ is due to its reaction with PdP$_2$. Because PdP$_2$ is a poorly soluble compound, the Pd(dba)$_2$ conversion takes place on the surface of nanosized palladium phosphide. It is the crossover of the reaction from homogeneous to heterogeneous kinetics that causes the sharp decrease in the reaction rate.

This hypothesis was verified by an X-ray diffraction analysis of the black precipitate forming in the Pd(dba)$_2$–0.2P system—sample **2** (Pd(dba)$_2$ conversion of 70%). According to X-ray diffraction data, this sample is a mixture of crystalline and amorphous phases (Fig. 6). Its diffraction pattern shows, against the background of an amorphous halo at 2θ = 30°–75°, reflections from the crystalline palladium phos-

phides PdP$_2$, Pd$_3$P$_{0.8}$, and Pd$_{4.8}$P. It is possible that the sample contains finely dispersed palladium. The palladium phosphide Pd$_3$P$_{0.8}$ is known to crystallize in a cementite-type (Fe$_3$C) structure. The difference between this phase and the ideal phosphide Pd$_3$P (Pd : P = 3 : 1) is due to random phosphorus vacancies [16]. A number of reflections from crystalline phases in the 2θ = 6°–30° range were not identified.

The presence of PdP$_2$ in sample **2** (P : Pd = 0.2) is consistent with the above hypothesis that, irrespective of the reactant ratio, the reaction between Pd(dba)$_2$ and white phosphorus proceeds via the formation of palladium diphosphide, which then reacts slowly with Pd(0) to yield palladium-rich phosphides. Bis(dibenzylideneacetone)palladium(0), whose empirical for-
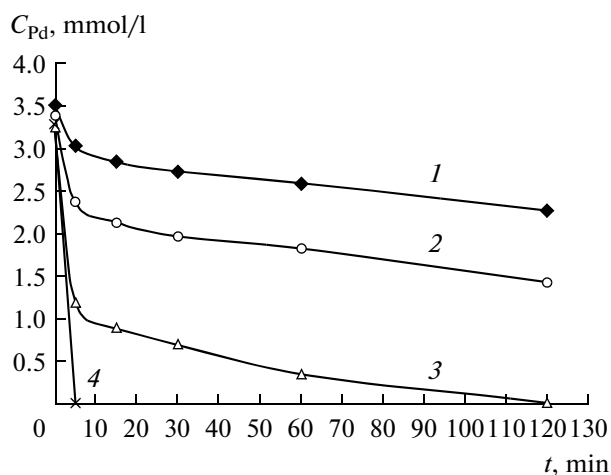

Fig. 5. Time variation of the Pd(dba)$_2$ concentration in the interaction between Pd(dba)$_2$ and white phosphorus in benzene at different reactant molar ratios: [P] : [Pd(dba)$_2$] = (*1*) 0.2, (*2*) 0.4, (*3*) 1.0, and (*4*) 2.0. $C_{\text{Pd(dba)2}}$ = 3.3 mmol/l, 20°C.
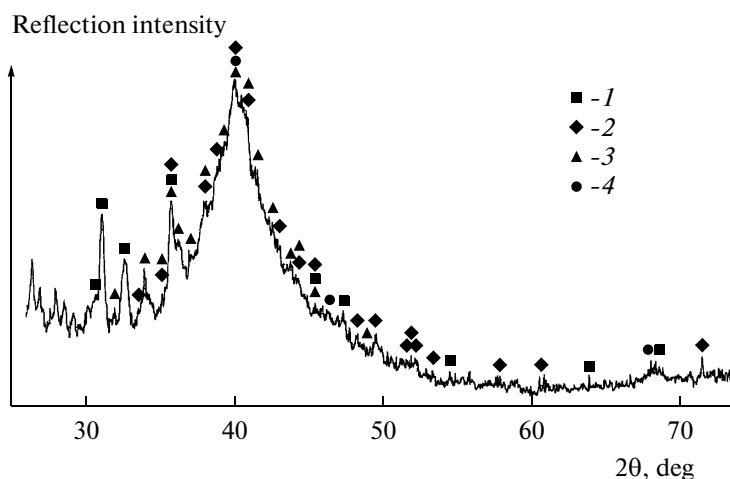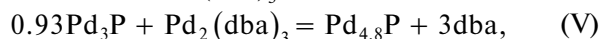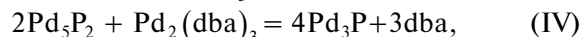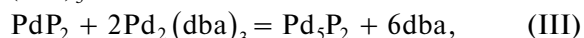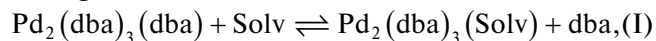
Fig. 6. X-ray diffraction patterns of sample **2** (P : Pd(dba)$_2$ = 0.2): (*1*) PdP$_2$, (*2*) Pd$_3$P$_{0.8}$, (*3*) Pd$_{4.8}$P, and (4) unidentified phase.

mula is Pd(dba)$_2$, is actually an M$_2$(dba)$_3$(dba)-type (M = Pd, Pt) dinuclear complex with three bridging dibenzylideneacetone ligands in s-*cis* and s-*trans* conformations, with the fourth dibenzylideneacetone molecule replacing the solvent molecule during recrystallization [17]. The formation of palladium phosphides can, therefore, be represented as the following consecutive reactions:

$$Pd_2(dba)_3(dba) + Solv \rightleftharpoons Pd_2(dba)_3(Solv) + dba, \quad (I)$$

$$Pd_2(dba)_3 Solv + P_4 = 2PdP_2 + 3dba + Solv, \quad (II)$$

$$PdP_2 + 2Pd_2(dba)_3 = Pd_5P_2 + 6dba, \quad (III)$$

$$2Pd_5P_2 + Pd_2(dba)_3 = 4Pd_3P + 3dba, \quad (IV)$$

$$0.93Pd_3P + Pd_2(dba)_3 = Pd_{4.8}P + 3dba, \quad (V)$$

where Solv = solvent.

It was demonstrated by additional experiments that PdP$_2$ indeed reacts with Pd(dba)$_2$ in benzene at room temperature at an initial rate of 7×10^{-7} mol l^{-1} min^{-1} ($C_{Pd(dba)_2}$ = 3.55 mmol/l, Pd(dba)$_2$: PdP$_2$ = 11). The above mechanism of palladium phosphides formation

as a result of the reaction between Pd(dba)$_2$ and phosphorus in benzene can likely be extended to the reaction taking place in DMF. The radical difference between the reactions occurring in these solvents is that palladium nanocluster formation in DMF is a side reaction. It is natural that the palladium phosphides forming in benzene and those forming in DMF may differ in composition at the same initial P : Pd ratio and reaction time because, in the case of DMF, part of the Pd(dba)$_2$ will turn into palladium nanoclusters by reacting with DMF and the P : Pd ratio in the solution will change. However, the sequence of elementary steps yielding palladium phosphides will be the same.

The above data suggest that the following two processes occur at a high rate in the Pd(dba)$_2$–P–styrene catalytic system at room temperature: chemical conversion of the Pd(dba)$_2$ complex into the phosphides PdP$_2$ and Pd$_5$P$_2$, which are inactive in hydrogenation under mild conditions [3], and Pd(dba)$_2$ conversion into palladium nanoclusters under the action of DMF and styrene:
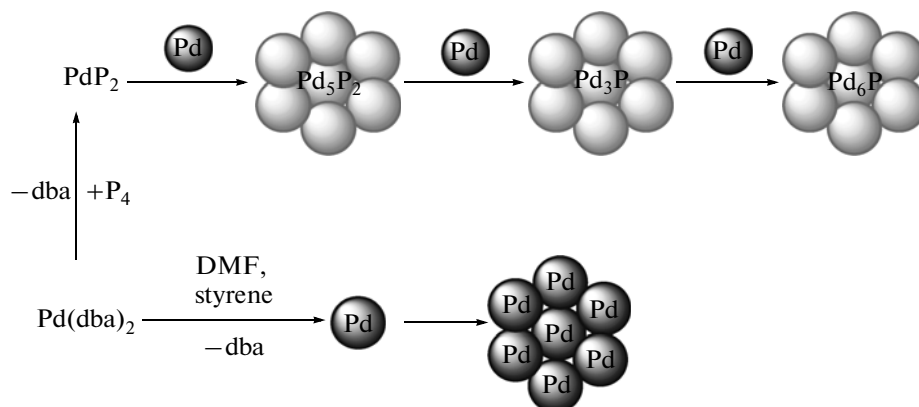
The fact that the catalytic activity is inversely proportional to the P : Pd ratio indicates that, upon the

introduction of phosphorus, part of the palladium turns into hydrogenation-inactive form. We think that

this is due to the dominant formation, under the catalytic conditions, of segregated nanoparticles of palladium phosphides, which are inactive in hydrogenation under mild conditions, and palladium nanoclusters. The segregation of the nanoparticles may be caused by the following two factors. The first is the high rate of $Pd(dba)_2$ conversion into palladium nanoclusters via the replacement of dibenzylideneacetone in the coordination sphere of palladium by the substrate (styrene), which alone is incapable of stabilizing mononuclear Pd(0) complexes, even though it is in large excess in the system. The second factor is the low rate of the chemical reaction between Pd(0) and PdP_2 (which results from the introduction of phosphorus into the system) yielding the palladium-rich phosphides Pd_5P_2, Pd_3P, and $Pd_{4.8}P$ via a number of consecutive steps. It is also possible that the interaction of Pd(0) with the palladium phosphides present in the solution yields core−shell type particles in which the core is Pd_xP and the shell is Pd(0). However, the proportion of these nanoparticles is likely small.

With the order in which the components were introduced into the solution (phosphorus and, after 10 min, styrene), the $Pd(dba)_2$ conversion into nanosized palladium phosphides and palladium nanoclusters depends on the P : Pd ratio.

Our investigation of the interaction between $Pd(dba)_2$ and elemental phosphorus verifies some steps of the above mechanism of the formation of the Pd(II)-based, phosphorus-modified, nanosized hydrogenation catalysts [3]. We hypothesized in our earlier work [3] that, depending on the ratio of the rates of Pd(II) reduction with phosphorus and hydrogen and the rate of subsequent nanoparticle growth, the process can yield nanoparticles consisting of palladium nanoclusters, palladium phosphide nanoparticles of various compositions, or core−shell nanoparticles. The high rate of Pd(II) reduction by hydrogen and, as a consequence, a high degree of supersaturation are favorable for Pd(0) nucleation via homogeneous condensation. In this case, at P : Pd < 1 a mechanical mixture of palladium phosphide nanoparticles and palladium nanoclusters will mainly form in the reaction system. The conversion of part of the palladium into hydrogenation-inactive phosphides will decrease the catalytic activity of the system at any reactant ratio; that is, phosphorus will act as a catalyst poison. This is the case in catalytic systems in which the palladium precursor is in the zero oxidation state (e.g., $Pd(dba)_2$) and in systems in which the Pd(II) compound is reduced at a high rate, for example, $PdCl_2–P–H_2$ [3] and $Pd(acac)_2–P–AlEt_3$ [18]. Note that, in these catalytic systems, owing to the high nucleation (Pd(II) reduction) rate, finely dispersed catalysts with a particle size of 3−5 nm form in the absence of phosphorus as well. If the rate of Pd(II) reduction with hydrogen is low, the heterogeneous

mechanism of Pd nucleation will dominate in the system. In this mechanism, the crystallization centers are nanoparticles of the poorly soluble palladium phosphides that form in the solution as a result of the redox reaction between Pd(II) and phosphorus. This situation is typical of $Pd(acac)_2$, which reacts readily with white phosphorus at room temperature to yield palladium phosphides and, because of its chelate structure, is reducible with hydrogen at a noticeable rate only at 80°C [2]. In this case, the palladium phosphide nanoparticles, serving as crystallization centers for the Pd(0) resulting from the hydrogenolysis of the remaining $Pd(acac)_2$, increase the degree of dispersion and, accordingly, the catalytic activity of the nanosized palladium-based hydrogenation catalyst.

Thus, this study of the properties and nature of the nanoparticles resulting from the interaction between the palladium(0) complex $Pd(dba)_2$ and white phosphorus and earlier experimental studies [2, 3] have provided an explanation and experimental substantiation for the diametrically opposite effects of white phosphorus on the catalytic properties of nanosized palladium-based hydrogenation catalysts.

REFERENCES

1. RF Patent 2 323 776, 2008.
2. Belykh, L.B., Skripov, N.I., Belonogova, L.N., Umanets, V.A., and Schmidt, F.K., *Kinet. Catal.*, 2010, vol. 51, no. 1, p. 42.
3. Skripov, N.I., Belykh, L.B., Belonogova, L.N., Umanets, V.A., Ryzhkovich, E.N., and Schmidt, F.K., *Kinet. Catal.*, 2010, vol. 51, no. 5, p. 714.
4. Gordon, A.J. and Ford, R.A., *A Handbook of Practical Data, Techniques, and References*, New York: Wiley, 1972.
5. Mitchell, J. and Smith, D., *Aquametry*, New York: Plenum, 1977.
6. Vul'fson, N.S., *Preparativnaya organicheskaya khimiya* (Preparative Organic Chemistry), Moscow: Khimizdat, 1959.
7. Dzhemilev, U.M., *Metallokompleksnyi kataliz v organicheskom sinteze: Alitsiklicheskie soedineniya* (Catalysis by Metal Complexes in Organic Synthesis: Alicyclic Compounds), Moscow: Khimiya, 1999.
8. Ukai, T., Kawazura, H., and Ishii, Y., *J. Organomet. Chem.*, 1974, vol. 65, p. 253.
9. Kawazura, H., Tanaka, H., Yamada, H., and Takahashi, T., *Bull. Chem. Soc. Jpn.*, 1978, vol. 51, no. 12, p. 3466.

10. Wiehage, G., Weibke, Fr., and Biltz, W., *Z. Anorg. Allg. Chem.*, 1936, vol. 228, p. 357.

11. *Powder Diffraction File, Hanawalt Search Manual: Inorganic Phases*, sets 1–42, Swarthmore: JCPDS, 1992.

12. Harley, P.D., Adar, F., and Gray, H.B., *J. Am. Chem. Soc.*, 1989, vol. 111, no. 4, p. 1312.

13. Pomogailo, A.D., Rozenberg, A.S., and Uflyand, I.E., *Nanochastitsy metallov v polimerakh* (Metal Nanoparticles in Polymers), Moscow: Khimiya, 2000.

14. Schmidt, F.K., *Fraktal'nyi analiz v fiziko-khimii geterogennykh sistem i polimerov* (Fractal Analysis in the Physical Chemistry of Heterogeneous Systems and Polymers), Irkutsk: Irkutsk. Gos. Univ., 2001.

15. Durand, J., Teuma, E., and Gómez, M., *Eur. J. Inorg. Chem.*, 2008, no. 23, p. 3577.

16. Andersson, Y., Rundqvist, S., Tellgren, R., and Thomas, J.O., *J. Solid State Chem.*, 1980, vol. 32, p. 321.

17. Rubezhov, A.Z., *Usp. Khim.*, 1988, vol. 57, no. 12, p. 2078.

18. Belykh, L.B., Titova, Yu.Yu., Umanets, V.A., and Schmidt, F.K., *Russ. J. Appl. Chem.*, 2006, vol. 79, no. 8, p. 1271.